Propagation of Uncertainty in Chemically Activated Systems

Ioannis P. Androulakis
Chemical and Biochemical Engineering Dept., Rutgers University, Piscataway, NJ 08854

Jeffrey M. Grenda and Timothy A. Barckholtz
Corporate Strategic Research, ExxonMobil Research and Engineering Company, Annandale, NJ 08801

Joseph W. Bozzelli
Chemistry Dept., New Jersey Institute of Technology, Newark, NJ 07102

DOI 10.1002/aic.10945
Published online July 17, 2006 in Wiley InterScience (www.interscience.wiley.com).

Chemically activated systems play an important role in combustion and atmospheric chemistry. The overall reaction paths exhibit complex pressure and temperature dependencies because each intermediate involves a coupled system of competing multistep isomerization, dissociation, and stabilization paths. A number of estimation techniques exist for deriving the required thermochemical and elementary kinetic input parameters for rate coefficient estimation. The availability of high-level ab initio methods promises to reduce the inaccuracies associated with older empirical methods. The objective of this study is to evaluate the importance of the various thermochemical parameters entering the rate coefficient calculation. We describe and illustrate a computational framework to quantify the functional relationship between the thermochemical properties and the macroscopic observables through appropriate response surface methods. The approach is demonstrated by analyzing the impact of thermochemical properties in estimating autoignition delays in propane oxidation. © 2006 American Institute of Chemical Engineers *AIChE J,* 52: 3246–3256, 2006
Keywords: chemical kinetics, autoignition, response surface, uncertainty propagation

Introduction

Important products from the oxidation of fuel are the initial radicals derived from the fuel itself. The subsequent elementary reactions of the radicals with molecular oxygen are complex and difficult to study experimentally. These reactions represent the principal pathways of the radical conversion in many hydrocarbon oxidation and combustion processes. Low-temperature oxidation of hydrocarbons (<800 K) is critically important in their use as fuels in internal combustion engines. A distinguishing feature of the low-temperature chemistry of many molecules is the *negative temperature coefficient* (NTC).[1] At very low temperatures, as the temperature is raised the ignition delay of a fuel is decreased and its rate of oxidation is increased. However, for many fuels, at a certain temperature the combustion reverses its course and the ignition delays become longer as the temperature is raised. At some higher temperature, the oxidation rate increases again and the ignition delay decreases. This complex phenomenon is illustrated in Figure 1 for propane,[2] which clearly indicates the reversal in fuel oxidation kinetics.

Detailed chemical kinetic models are being increasingly

This article includes Supplementary Material available from the authors upon request or via the Internet at http://www.interscience.wiley.com/jpages/0001-1541/suppmat/.

Correspondence concerning this article should be addressed to I. P. Androulakis at yannis@rci.rutgers.edu.

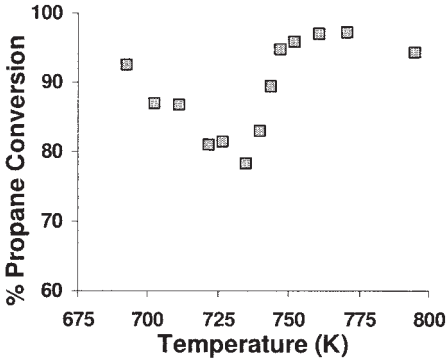

Figure 1. Propane conversion through the negative temperature coefficient (NTC).

Propane conversion as a function of initial temperature after 198 ms of reaction time. (From Koert et al.[51])

used for analysis and development of next-generation combustion devices. These models require a great deal of information to construct, and a number of straightforward techniques exist for deriving approximate values of that information.[3-6] The availability of high-level ab initio methods should reduce the inaccuracies associated with the various empirical methods.[7] A recent comprehensive study[8] demonstrated the potential of deriving much of the necessary input from first-principles calculations without the need for significant parameter adjustments.

However, quite often large uncertainties remain in the estimation of the fundamental thermochemical properties, given that the required accuracy of calculation is not always achievable. It was recently shown[1] that even variations in the energy calculations within the expected accuracy of quantum chemical calculations could lead to significant variations of the model predictions. The impact of small changes in high-pressure rate coefficients on the autoignition delay of propane is substantial.[2] Elsewhere,[9] the uncertainty of a single reaction ($CO + OH \rightarrow CO_2 + H$) in predicting CO_2 emissions in a supercharged engine was described. These two calculations illustrate the impact of variability in fundamental thermochemical properties on the prediction of macroscopic responses.

The focus of this article is to develop a rigorous method to quantify the impact of that uncertainty on macroscopic observables of combustion and fuel oxidation. The effects of uncertainty in thermochemical properties in the estimation of reaction rates and macroscopic properties are quantified using *response surface methods*. In particular, using the oxidation of three model systems (CH_3, C_2H_5, C_3H_7) as our motivation and focusing on the uncertainty in high-pressure rate constants, the following questions pertaining to both microscopic (rates) and macroscopic (ignition delay) observables are addressed:

- What is the expected range variability of apparent reaction rates given uncertainty in high-pressure rate constants?
- Which of the high-pressure rate constants are less influential in estimating apparent reaction rates and thus require less accurate estimation?
- Which of the high-pressure rate constants have the greatest impact on macroscopic observables, that is, ignition delay?

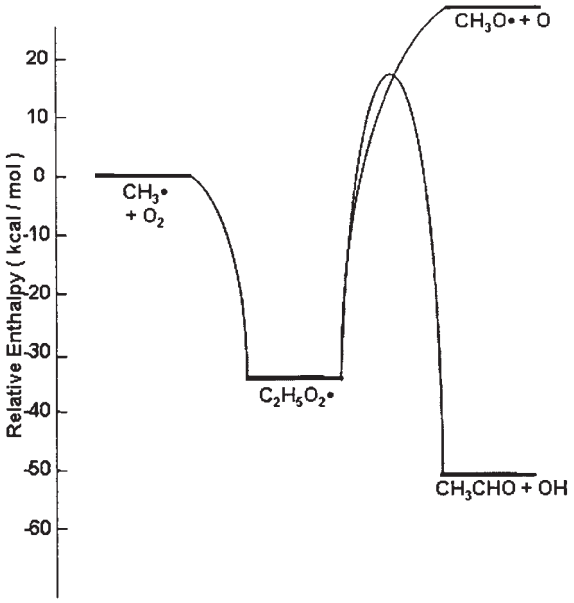

Figure 2. Potential energy diagram for the reaction of $CH_3 + O_2$.

Mechanism of NTC Behavior: Peroxy Radical Chemistry

The key species for modeling the NTC of alkanes are the peroxy radicals and their isomers. Propane is the smallest fuel that has an unambiguous NTC, whereas methane and ethane do not. These three fuels therefore form a simple progression in NTC behavior, yet remain small enough to be tractable. Simplified potential energy diagrams of the addition of O_2 to form the relevant hydrocarbon radicals for these fuels are illustrated in Figures 2–4, and rate coefficients for the elementary reactions are collected in Table 1.[2,10]

The relative rate of isomerization of the peroxy radicals to the concerted elimination[8,11] of HO_2· is the key to properly capturing the NTC behavior. By the addition of a second O_2, the CH_2·CH_2CH_2OOH isomer readily promotes chain branch-

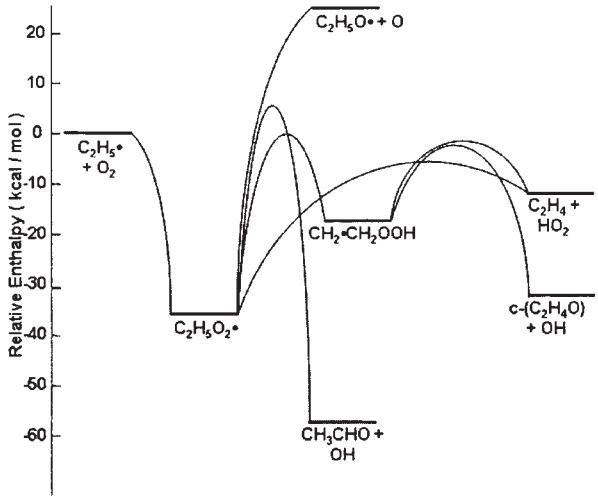

Figure 3. Potential energy diagram for the reaction of $C_2H_5 + O_2$.

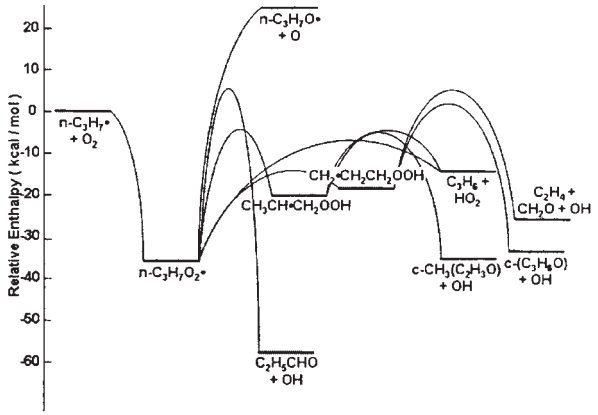

Figure 4. Potential energy diagram for the reaction of n-C_3H_7 + O_2.

This diagram contains only the most important reactions of the entire system. Table 1 gives the complete description in numerical format. An equivalent diagram exists for the i-C_3H_7 + O_2 system. However, this system does not have a significant impact on the NTC of propane and is not relevant to the current discussion.

ing and therefore accelerates the chemistry at low temperatures. In the NTC range, however, the concerted HO_2· elimination pathway from $CH_2CH_2CH_2OO$· radical becomes faster, which reduces the concentration of CH_2·CH_2CH_2OOH, and thus reduces chain branching. Additionally, the HO_2· radicals are reasonably stable, and have a fast self-reaction to produce H_2O_2 and O_2, which is chain terminating. Therefore, the NTC is the manifestation of the subtle balance between chain branching and chain termination, as mediated by the peroxy radical chemistry.

Elsewhere,[2] a detailed mechanism with 216 species and 3078 reactions was developed to simulate numerous low-temperature experiments of propane oxidation, one example of which is given in Figure 1. In that work, ab initio calculations were used to develop initial estimates of the peroxy radical kinetics. Despite the high quality of the calculations, two key activation energies had to be adjusted by 8 kJ/mol each to achieve good agreement with experimental data. These adjustments were well within the expected accuracy of the calculations. Those adjustments were made empirically to obtain a good fit to the data. One of the key goals of the work reported herein is to quantify the propagation of the uncertainty of the ab initio properties into the final macroscopic observable, such as ignition delay or conversion amount.

Chemically Activated Reactions

There is an additional complication in the use of ab initio calculations for the prediction of kinetic rate coefficients. Many gas-phase reactions, including those of the peroxy radicals (Table 1), are pressure dependent. By application of statistical mechanics, the ab initio calculations produce good estimates of the *high-pressure limit* of the *elementary* rate coefficients. Furthermore, a complex reaction network like those shown in Figures 2 to 4 contains numerous *apparent* rate coefficients, in which multiple elementary steps (Table 1) are—in one reaction "step"—combined to yield an apparent rate coefficient. For example, the ab initio calculation can give the high-pressure rate coefficients for the reactions C_2H_5· + O_2 = C_2H_5OO· and C_2H_5OO· = C_2H_4 + HO_2·, although in actual simulations the rate coefficients of the direct reaction C_2H_5· + O_2· = C_2H_4 + HO_2·, and all other permutations, are needed as a function of both temperature and pressure. Compound rate expressions can be derived by application of the steady-state approximation, but this is not a universal route to rate coefficient expressions and does not yield pressure-dependent rate coefficients.

Existing kinetic model construction algorithms are based on a series of rules that describe known reaction steps. Numerous algorithms that identify and manage reactant and product spe-

Table 1. High-Pressure Rate Coefficients for the Reactions of CH_3, C_2H_5, and n-C_3H_7 with O_2*

No.	Reaction	A	n	E_a
	CH_3 + O_2			
1	CH_3· + O_2 = CH_3OO·	1.07×10^9	1.31	12.5
2	CH_3OO· = CH_2O + OH·	4.60×10^{13}	0.0	209.2
3	CH_3OO· = CH_3O· + O	7.2×10^{14}	0.0	251.0
	C_2H_5 + O_2			
4	C_2H_5· + O_2 = C_2H_5OO·	2.94×10^{13}	−0.44	0.0
5	C_2H_5OO· = CH_2·CH_2OOH	7.90×10^6	1.79	149.9
6	C_2H_5OO· = CH_3CHO + ·OH	1.32×10^9	1.37	174.0
7	C_2H_5OO· = C_2H_4 + HO_2·	8.80×10^5	2.243	123.9
8	C_2H_5OO· = C_2H_5O· + O	2.98×10^{15}	−0.09	257.7
9	CH_2·CH_2OOH = C_2H_4 + HO_2·	1.28×10^{11}	0.519	67.7
10	CH_2·CH_2OOH = c-(C_2H_4O) + OH·	1.32×10^{10}	0.716	64.5
	n-C_3H_7 + O_2			
11	n-C_3H_7· + O_2 = C_3H_7OO·	2.94×10^{13}	−0.44	0.0
12	C_3H_7OO· = CH_3CH·CH_2OOH	2.10×10^7	1.29	131.0
13	C_3H_7OO· = CH_2·CH_2CH_2OOH	4.79×10^6	1.39	87.7
14	C_3H_7OO· = C_3H_6 + HO_2·	1.89×10^7	1.51	115.6
15	C_3H_7OO· = C_2H_5CHO + OH·	1.14×10^9	1.15	172.6
16	C_3H_7OO· = C_3H_7O· + O	2.98×10^{15}	−0.09	257.7
17	CH_3CH·CH_2OOH = c-CH_3(C_2H_3O) + OH·	8.54×10^8	0.85	60.7
18	CH_3CH·CH_2OOH = C_3H_6 + HO_2·	6.74×10^9	0.67	63.9
19	CH_2·CH_2CH_2OOH = c-(C_3H_6O) + OH·	1.26×10^{10}	0.37	84.5
20	CH_2·CH_2CH_2OOH = C_2H_4 + CH_2O + OH·	1.06×10^{12}	0.57	112.1

Units: A, cm^3 mol^{-1} s^{-1}; E_a, kJ/mol; $k = AT^n e^{-E_a/RT}$.

cies exist in the literature.[12-20] Rate coefficients are often expressed in a modified Arrhenius form ($k = AT^n e^{-E/RT}$) on the basis of experimental data, quantum chemical calculations, or Evans–Polanyi correlations. For combustion chemistry applications, chemically activated reactions play an important role[21] but present additional modeling challenges. Such reactions involve highly energized (nonthermalized) species that undergo rapid isomerization, dissociation, or collisional stabilization. The energized intermediates are sufficiently short-lived that these reactions can be modeled as direct reactions between the thermalized species, although the chemical structure changes between reactants and products reflect the multistep nature of the process.

In the example of Figure 4, the entrance species, propyl and oxygen, form a highly energized $CH_3CH_2CH_2OO\cdot$* adduct, which can subsequently be collision stabilized and form the peroxy radical ($CH_3CH_2CH_2OO\cdot$) or react according to any of the remaining steps. However, when building the apparent mechanism only stabilized adducts and molecular species are included. Because each energized intermediate adduct involves a coupled system of competing multistep isomerization and stabilization pathways, the overall rate coefficients for the apparent reactions exhibit complicated pressure and temperature dependencies. For a computer algorithm to construct accurate kinetic models, these chemically activated processes should be included in the construction process.

The apparent rate coefficients of these pressure-dependent reactions can be evaluated by combining the rate coefficients at high pressure with any of a variety of methods and appropriate treatments of collision stabilization, such as the modified strong collision theory[22] or the master equation.[1] The high-pressure rate coefficients that are formulated as a function of temperature need to be converted to microcanonical rate coefficients that are functions of internal energy, using either the Rice–Rampserger–Kassel (RRK) or Rice–Rampserger–Kassel–Marcus (RRKM) theory.[4,21,23,24] An efficient quantum RRK (QRRK) has been described[25,26] and its implementation (CHEMACT[27]) makes use of the modified strong collision approximation. The required input parameters for these calculations include: the high-pressure rate coefficients (A^∞, n^∞, E^∞) for all elementary reactions; the $\Delta_f H_{298}$, S_{298}, and $C_p(T)$ for each stable species; the Lennard–Jones parameters describing the interaction between the stable species and the bath gas; and a parameterization of the collision energy between the stable species and the bath gas. We have used CHEMACT for this work because, relative to the master equation codes, it offers a tremendous advantage in speed with only a marginal debit in accuracy.

A computational necessity is to have a closed form of the pressure and temperature dependencies of the apparent reaction rate coefficients of the system. Many methods have been proposed to achieve this goal, including the formulas of Troe[28] and, more recently, the use of Chebyshev polynomials.[29] The commonly used Troe formula does not have sufficient flexibility to describe the rate coefficients computed on a complex potential energy surfaces such as that of Figure 4 and Reactions 11–20 of Table 1. The Chebyshev polynomials, although very flexible and accurate over a wide temperature and pressure range, are complicated to use and have coefficients with little physical meaning.

In the current work, the rate coefficients $k(T, P)$ are fitted according to a polynomial expansion based on the modified Arrhenius expression:

$$k(T,P) = A_P T^{n_P} e^{-E_P/RT} \tag{1}$$

where A_P, n_P, and E_P are each expressed as a quadratic function of $\log_{10}P$ (with P in atm):

$$\log_{10}[A_P(P)] = a_0 + a_1\log_{10}P + a_2\log_{10}^2P$$

$$n_P(P) = n_0 + n_1\log_{10}P + n_2\log_{10}^2P$$

$$E_P(P) = e_0 + e_1\log_{10}P + e_2\log_{10}^2P \tag{2}$$

All nine coefficients of this expression are fitted to the $k(T, P)$ computed from the pressure-dependent code using a nonlinear least-squares algorithm, typically over the range from 500 to 2000 K and from 1 to 100 atm. The residual error in the fit is typically $<10\%$ and often considerably better. Although this polynomial form does not have rigorously correct low- and high-pressure limits such as the Troe formula, it is a very compact and easily computable formula. Finally, the coefficients a_0, n_0, and e_0 by themselves generate the rate coefficient expressions at $P = 1$ atm, which is a convenient pressure for which to have an easily read rate coefficient expression.

Quantifying the Impact of Thermochemical Properties on Macroscopic Observables

It is important to evaluate the impact of "uncertainty" (measure of the error arising from the calculation) in the fundamental properties that enter the microscopic rate calculations. A comprehensive study was recently performed to evaluate the thermochemical properties of species involved in the reactions of vinyl and phenyl radicals systems with oxygen,[31] showing that a change of only 1.0 to 1.5 kcal mol^{-1} in a barrier (transition state structure energy) controlled the balance between branching and termination. To address these issues we treat the thermochemical properties that are the input to the rate coefficient calculations algorithms, that is, CHEMACT,[23,24,32] as *uncertain parameters*. An uncertainty for each of these properties is estimated, and reactive flow calculations are performed to determine the propagation of that uncertainty to the final observed property of interest, such as an ignition delay time.

In the context of the framework we just described, let Y be the set of macroscopic observables of interest and let Z represent the various primary parameters (high-pressure rate coefficients, etc.). We are interested in the analysis of the relationship $Y = Y(Z_i)$. In particular we consider two kinds of observables: (1) reaction rate coefficients, $k(T, P)$, generated from CHEMACT; and (2) autoignition delays based on a reactive flow simulation. Local sensitivity analysis, normally not performed on the primary parameters, could be used to evaluate the uncertainty in Y as a result of small variations in Z about a "reference" point.

For a linear problem the sensitivity, appropriately weighted by the variance on Y as a result of variance in Z, could be used to quantify the impact on Y:

$$Y(Z_i) = \sum_{i=1}^{r} \Omega_i Z_i \Rightarrow S_{Z_i}^{\sigma} = \frac{\sigma_{Z_i}}{\sigma_Y}\frac{\partial Y}{\partial Z_i} = \Omega_i \frac{\sigma_{Z_i}}{\sigma_Y} \qquad (3)$$

The weighting is important because otherwise the sensitivity defined as simply the partial derivative would overemphasize variables with large coefficients (Ω_i) in the model, even though they may exhibit very small variations (small σ_{Z_i}). Sensitivity analysis has found many applications with significant implications in a number of areas such as chemical kinetics[33-35] and atmospheric chemistry.[36]

The complication with "global" sensitivity is that we should consider variations not only around the nominal value but also across the entire range of values, which must be properly accounted for and weighted. If the problem is linear and the characteristics of the distribution of the inputs are known (mean, standard deviation, and so on) then the equations just described would answer, to some extent, the problems we put forth earlier. However, for general nonlinear problems derivatives can no longer provide the required information and "exploration"-type approaches are required to optimally map the input space and generate the required statistics for the output variables.[37] A number of sampling methods have been proposed in the literature to address this type of problems. The following are three among the leading candidate methods:

1. Monte Carlo (MC) and Latin Hypercube Sampling (LHS). These have found a wide range of applications in numerous areas.[38,39]

2. Fourier Amplitude Sensitivity Test (FAST).[40] This method is based on a Fourier transformation of the uncertain model parameter space into a frequency domain, thereby reducing the multidimensional model into a single dimensional.

3. Response Surface Methods (RSMs). These methods basically consist of making multiple, but optimally selected, runs of the computer model using specific values and combinations of the input variables to sample the input space according to the expected uncertainty characteristics. An appropriate polynomial form is fitted to the data and all inferences related to uncertainty/sensitivity characteristics of the system's output are derived from the analysis of the fitted model. Numerous implementations have been proposed in the literature.[41,42]

A key advantage of the RSM over the other methods is that a potentially intensive model can be reduced to a simplified form that enables much faster model run times. It was recently demonstrated[43] how to combine RSMs and automatic differentiation (ADIFOR) of the resulting FORTRAN code to significantly enhance the sensitivity analysis of the resulting surface.

Our results are based on the RSM because of the increased computational efficiency and the ability of the RSM to generate a surrogate model for further analysis, as opposed to merely producing the overall statistics of the system's output.

Modeling aspects of the approach

Figure 5 summarizes the basic steps on the forward calculation. Electronic structure calculations or other methods generate the input data required by the pressure-dependent code (CHEMACT). The $k(T, P)$ values are fitted to modified Arrhenius expressions and all the derived channels are assembled to a kinetic mechanism, which is augmented by non-pressure-dependent rate coefficients assembled with other methods. This mechanism is used to make macroscopic predictions of bulk observables. Our results focus on autoignition delay.

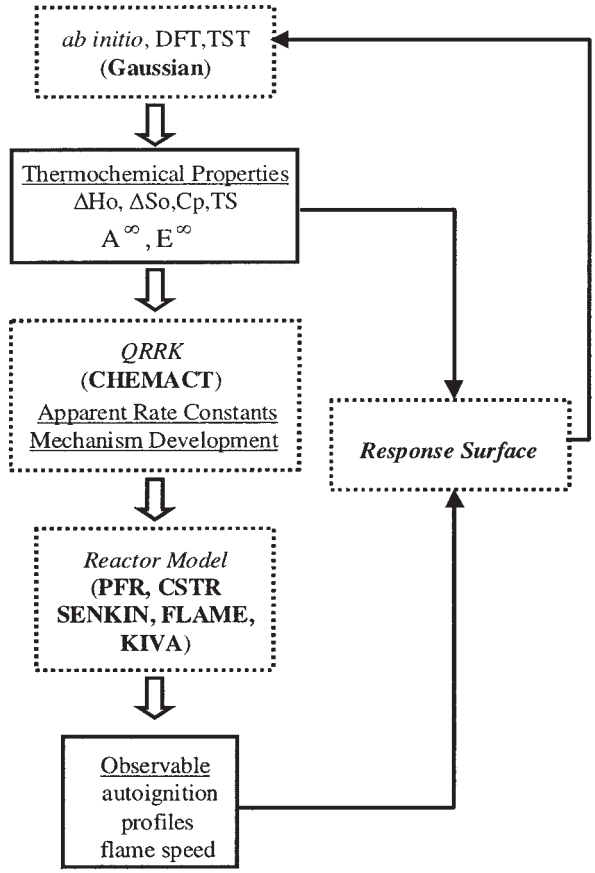

Figure 5. Framework for the integration of uncertainty propagation in pressure-dependent rate coefficient calculations with a response surface.

To quantify the functional relationship between the thermochemical properties and the macroscopic observables the definition of a response surface is used. In particular the *stochastic response surface method* (SRSM)[43] was used and integrated with CHEMACT. SRSM uses computationally efficient instantiations of the input variables responsible for the variability. Based primarily on the *deterministic equivalent modeling method*,[44,45] SRSM expresses random outputs in terms of the polynomial chaos expansion[46] of Hermite polynomials and the implementation uses an efficient collocation scheme combined with regression to determine the coefficients of the expansion. The original random variables are appropriately transformed based on their respective distribution. The transformation depends of the distribution of the input variables. For uniformly distributed random variables in the range $[a, b]$, which are assumed in this study, the transformed variables are given by $a + (b - a)[\frac{1}{2} + \frac{1}{2}\,\mathrm{erf}(z/\sqrt{2})]$, where z is normal $\mathcal{N}(0, 1)$.

Functional forms of the expansion, in terms of transformed variables, for a first-, second-, and third-order polynomial approximation are

$$U_1 = a_{0,1} + \sum_{i=1}^{n} a_{i,1}\xi_i U_2 = a_{0,2} + O(1)$$

$$+ \sum_{i=1}^{n} a_{ii,2}(\xi_i^2 - 1) + \sum_{i=1}^{n-1}\sum_{j>i}^{n} a_{ij,2}\xi_i\xi_j U_3 = a_{0,3} + O(1) + O(2)$$

$$+ \sum_{i=1}^{n} a_{iii,3}(\xi_i^3 - 3\xi_i) + \sum_{i=1}^{n}\sum_{j=1}^{n} a_{ijj}(\xi_i\xi_j^2 - \xi_i)$$

$$+ \sum_{i=1}^{n-2}\sum_{j>i}^{n-1}\sum_{k>j}^{n} a_{ijk}\xi_i\xi_j\xi_k \quad (4)$$

This polynomial form possesses several useful properties including straightforward determination of the statistics of the output distribution. Although other response surface methods[47] are similar in spirit, SRSM offers the advantage that the probability density functions of the output metrics better approximate the actual distribution of the output parameters.[48] The integrated SRSM/CHEMACT framework permits—through the analysis of a minimal number of calculations—the development of quantitative models that identify (1) critical pathways within a given potential energy surface and (2) critical thermochemical data that influence model predictions.

Following its construction, the response surface can be used as a surrogate model of the complicated, expensive model. Additionally, the coefficients of the approximation can be used explicitly to derive the statistics of the output distribution. In particular, the standard deviation (SD) of the output can be estimated based on the second-order polynomial parameters:

$$\text{mean} = a_{0,z} \qquad \text{SD} = \sqrt{\sum_{i=1}^{n} a_{i,2}^2 + 2\sum_{i=1}^{n} a_{ii,2}^2} \quad (5)$$

Previous formalisms of response surface–based methods aiming at analyzing reactive simulations have focused on the impact of macroscopic parameters such as apparent kinetic rate coefficients and heats of formation entering the heat balance and not the estimation of the kinetic parameters.[49,50] Although such an approach can provide critical information regarding the sensitive components of the model, it does not provide any guidance as to whether or how the observed uncertainties can be reduced or what their fundamental cause is. In contrast, the current, integrated methodology identifies the fundamental sources of uncertainty and evaluates the true impact of the associated parameters. Furthermore, this type of multiscale uncertainty propagation provides guidance as to the required course of action for reducing uncertainty, as opposed to simply identifying the important manifestations thereof. Finally, because our methodology determines the impact of fundamental properties based on their expected range of variability, it can assess whether experimental observations can be explained/reconciled by updating the parameter estimates or whether the structure of the model should be questioned and improved.

In the following sections, the uncertainty propagation is demonstrated for the three systems of Figures 2 to 4. The first two examples focus on the uncertainty propagation in the rate coefficients $k(T, P)$ in the systems $CH_3 + O_2$ and $C_2H_5 + O_2$. In contrast, the third example does not stop at propagating the error into only $k(T, P)$, but demonstrates the uncertainty propagation from the high-pressure rate coefficient expressions of Table 1 all the way to the macroscopic observable of ignition delay.

Expected Variability of Kinetic Rate Coefficients: $CH_3 + O_2$

This is a simple, single-well system (Figure 2) for which reliable rate coefficients exist and which has been extensively studied in the open literature.[26] It is important because the reactions of the methyl radical are critical in combustion. We performed the analysis assuming that the uncertain parameters included.

High-Pressure Preexponential of the Entrance Channel

$$CH_3 + O_2 \xrightarrow{k_1} CH_3OO$$

The Heat of Formation of CH_3OO

The High-Pressure Preexponential of the Dissociation Reaction

$$CH_3OO \xrightarrow{k_3} CH_3O + O$$

The High-Pressure Preexponential and Activation Energy of Reaction

$$CH_3OO \xrightarrow{k_2} CH_2O + OH$$

Modified Arrhenius expressions are assumed ($k_i = A_i T^{n_i} e^{-E_i/RT}$, $i = 1, 3, 4$). The high-pressure rate coefficients of the steps shown graphically in Figure 2 and numerically in Table 1 were all treated as uncertain parameters uniformly distributed within the ranges: within the ranges: $A^\infty = [0.3A^\infty_{\text{nominal}}, 3A^\infty_{\text{nominal}}]$, $E^\infty = E^\infty_{\text{nominal}} \pm 3$ kJ/mol as well as uncertainty of ± 12 kJ/mol in the enthalpy of formation of CH_3OO.

The analysis was performed parametrically in T. Using the SRSM model, we performed a Monte Carlo sampling to assess the expected variability in the rate coefficients (Figure 6). The temperature-dependent analysis of linear coefficients of the quadratic SRSM model identifies the key contributors, that is, parameters whose variability mostly influences the prediction.

For the reaction $CH_3OO = CH_3O + O$, Figure 6a demonstrates how the propagated uncertainty depends on temperature. At high temperatures, this reaction has a very fast rate coefficient that is largely independent of uncertainty in the elementary rate coefficients. However, at low temperatures a broader distribution of potential rate coefficients is observed. The uncertainty in the outcome clearly depends on the conditions of interest. At high temperatures, this rate coefficient would be observed to be well known, whereas at low temper-

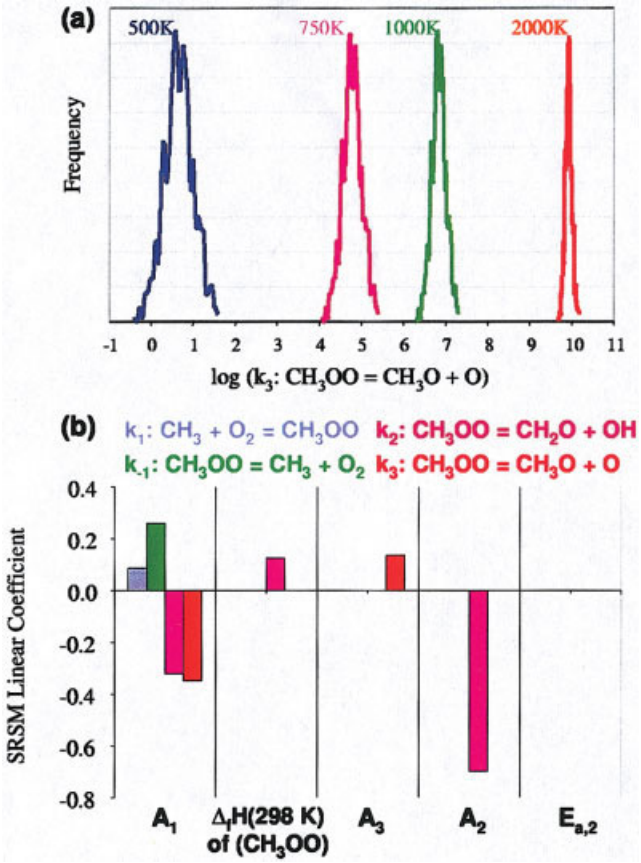

Figure 6. Propagation of uncertainty in $CH_3 + O_2$ system into $k(T, P)$.

(a) Histograms for the calculated values of $k(T, 1\ \text{atm})$ for the reaction $CH_3OO = CH_3O + O$. At high temperature, a more narrow range is observed than at low temperature, indicating how the uncertainty propagation depends on the conditions of interest. (b) SRSM coefficients for four apparent reaction rate coefficients in the system. The entrance rate coefficient (A_1, Table 1) has an impact on all rate coefficients, whereas each other uncertain parameter has an impact on only one or no rate coefficients. [Color figure can be viewed in the online issue, which is available at www.interscience.wiley.com]

atures, this rate coefficient could be viewed as being highly uncertain.

The linear coefficients at 500 K are summarized in Figure 6b. Overall we have identified limited sensitivity to variation in most of the parameters attributed to the existence of high barriers for all exit pathways (except reverse dissociation). If a reaction has a high barrier that cannot be surmounted at a low temperature, then the uncertainty in this barrier, although it may be large from the perspective of a quantum chemical calculation, translates into a low uncertainty of the computed rate coefficient. Essentially, the barrier is never low enough to increase the reaction rate coefficient, and thus the SRSM coefficients are small. However, the entrance barrier has a low barrier, and thus all rate coefficients depend critically on it.

Expected Variability of Kinetic Rate Coefficients: $C_2H_5 + O_2$

This reaction system represents an important model system to explore the kinetic consequences of the reaction of hydrocarbon radicals with molecular oxygen. It contains many of the complexities of larger systems yet is amenable to higher-level electronic structure calculations. Furthermore, it has been studied extensively experimentally. Figure 3 depicts the potential energy diagram[8] of the system. Despite the apparent simplicity of the system, a critical step—direct HO_2 elimination from the ethylperoxy adduct (by transition state TS1)—was only recently characterized.[11] It was shown that this path was not only energetically preferred but also it was the only consistent way of explaining experimental observations.[22]

The high-pressure rate coefficients of the steps shown graphically in Figure 3 and numerically in Table 1 were all treated as uncertain parameters uniformly distributed within the ranges: $A^{\infty} = [0.3A^{\infty}_{\text{nominal}}, 3A^{\infty}_{\text{nominal}}]$ and $E^{\infty} = E^{\infty}_{\text{nominal}} \pm 3$ kJ/mol. (The values of n^{∞} remained fixed.) The results (Figure 7b) indicate that the indirect channels exhibit a much greater effect in terms of input parameter uncertainty. The indirect HO_2 elimination channel needs to cross two transition states (TS2 and TS3) and therefore multiple factors can contribute to the expected kinetics. The direct channel, going through TS1, although it is the dominant channel, $k_{\text{direct}}(T, P) \gg k_{\text{indirect}}(T, P)$, exhibits much smaller variability in terms of the range of expected values.

This is quantified by estimating the standard deviation of the k values and we observe that $\sigma_{\text{indirect}} > \sigma_{\text{direct}}$. The latter is calculated by sampling the input space (1000 Monte Carlo runs of the CHEMACT code sampling the possible values of the high-pressure rate parameters) followed by application of Eq. 4. The plot depicts the excellent prediction of the variance of the output variables by directly estimating the standard deviation using the coefficients of the second-order SRSM approximation.

This analysis demonstrated that the uncertainty in the high-pressure rate coefficients propagates to a large uncertainty in the value of k_{indirect}. However, k_{indirect} is typically 100 times slower than k_{direct}; thus, a large uncertainty in k_{indirect} may still leave it as a very unimportant reaction in comparison to k_{direct}. Had we performed a sensitivity analysis of some macroscopic characteristic of the system we would likely conclude that k_{direct} is highly sensitive for the system. In other words, the macroscopic observable of the system (ignition delay) is more sensitive to k_{direct} than it is to k_{indirect}, despite the greater uncertainty of k_{indirect}.

In the next section, we illustrate the uncertainty propagation from the high-pressure rate coefficients through the pressure-dependent rate coefficient expressions and on to a macroscopic observable of ignition delay.

Expected Variability of Macroscopic Observables: $C_3H_7 + O_2$

The previous examples demonstrate that the activated and stabilized peroxy and hydroperoxy adducts have access to a number of reaction paths. These reactions become particularly important in the analysis of low-temperature autoignition exhibiting the NTC behavior. Propane oxidation is an excellent model system for this type of analysis for which noticeable NTC behavior has been reported in the literature. Using this system, we now demonstrate the propagation of quantum chemical calculation "errors" through a complete simulation predicting a macroscopic observable.

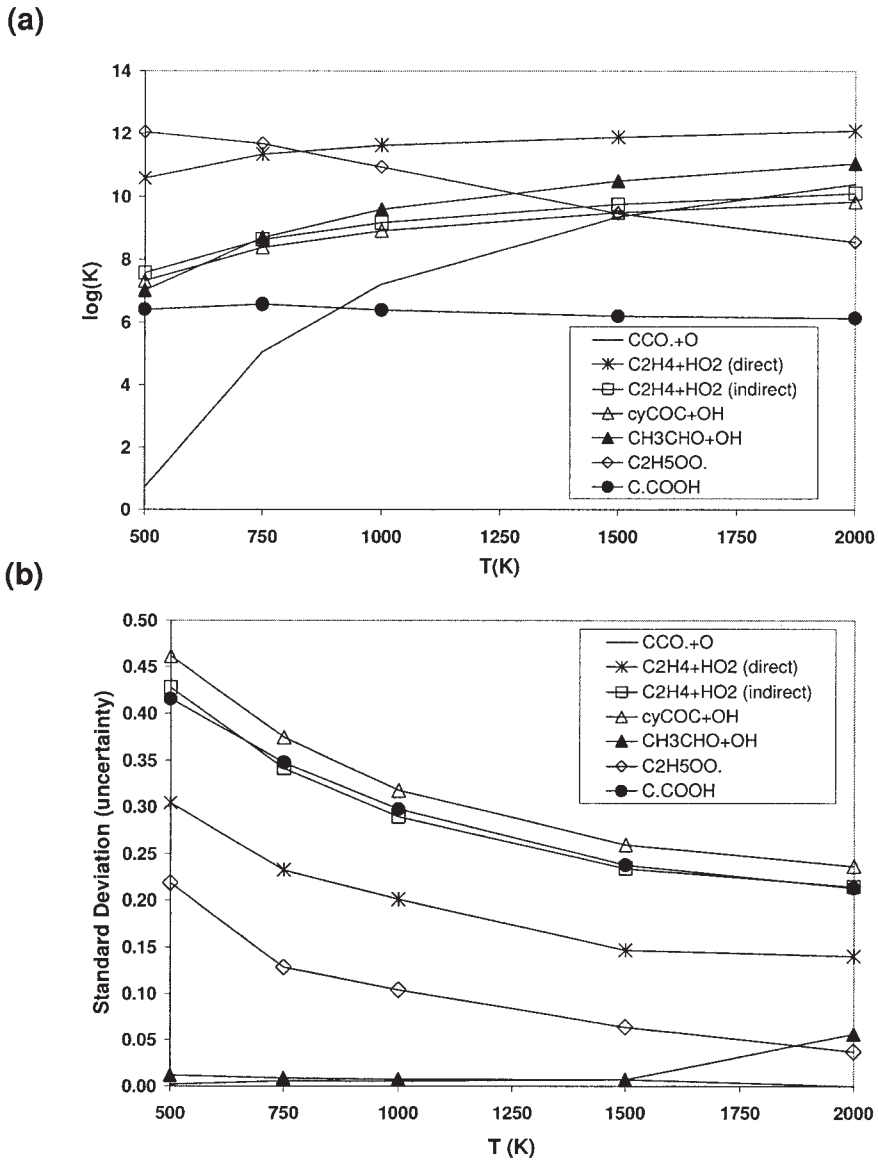

Figure 7. Propagation of uncertainty in $C_2H_5 + O_2$ system into $k(T, P)$.

(a) The apparent rate coefficients for the reaction of C_2H_5 with O_2 at 1 atm. (b) The uncertainty of the apparent rate coefficients over the range of input variability that was considered.

The potential energy diagram of the addition of oxygen to the *n*-propyl radical is depicted in Figure 4. The high-pressure rate coefficients (Table 1) are considered to be uncertain and for the purpose of our analysis we consider the uncertainty bounds to be the same as those for the $C_2H_5 + O_2$ system, above. Even for a "small" hydrocarbon molecule, such as propane, a detailed kinetic mechanism (216 species, 3078 reactions)[2] is required to accurately predict the experimentally observed "negative temperature coefficient" behavior.

The effect of the expected variability can be substantial, as shown in Figure 8, which reproduces the low-pressure static reactor data.[2] The range of uncertainty considered was the same as that for the $C_2H_5 + O_2$ case. One should notice that the NTC behavior cannot be correctly predicted under certain values of (A^∞, n^∞, E^∞), which are well within the expected range of calculation accuracy. The solid line denotes the nominal parameter value model estimates, using the values from Table 1, whereas the various points correspond to the estimated ignition delay if we assume "errors" in the nominal high-pressure rate coefficients (A^∞, E^∞).

The obtained SRSM model of the autoignition delay was able to correctly identify the critical dependency of the delay on the isomerization and HO_2 elimination steps in the NTC regime (580–650 K). For illustration purposes we summarize the linear SRSM coefficients, $\tau = a_1 A_1^\infty + \sum_{i=2}^{10} a_i A_i^\infty + b_i E_i^\infty$, in Table 2. The analysis is performed at three different temperatures (573, 593, and 683 K), which are selected because they correspond to the same macroscopic observable (autoignition delay $\approx$ 350 s; Figure 8, solid circles). At 573 K low-temperature chemistry dominates, at 593 K the oxidation has entered the NTC regime, whereas at 683 K high-temperature chemistry takes over. Even though the macroscopic be-

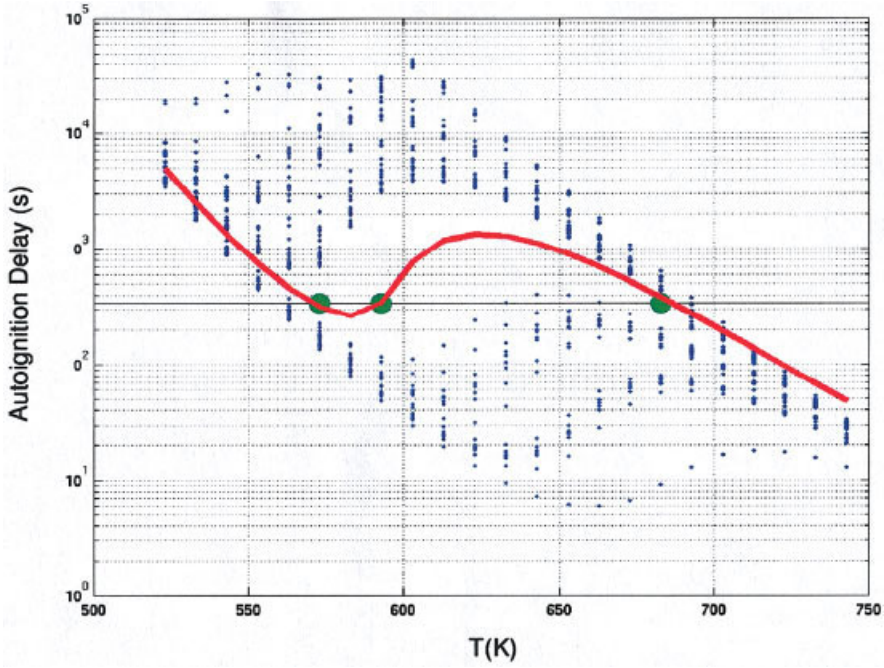

Figure 8. Propagation of uncertainty in $C_3H_7 + O_2$ system into the ignition delay of propane.

The center line indicates the computed ignition delay for the original, unperturbed model. Each circle represents a computed ignition delay for a model with a high-pressure input parameter adjusted within its uncertainty. [Color figure can be viewed in the online issue, which is available at www.interscience.wiley.com]

havior of the system is identical, the chemistry that gives rise to this behavior is distinctly different for each of the three initial temperatures.[30] The following observations can be made from Table 2:

(1) The isomerization (Reaction 13) and the direct HO_2 elimination (Reaction 14) are the dominant competing (branching vs. termination) contributors in the low-temperature chemistry regime, as their corresponding SRSM coefficients indicate. Increasing the high-pressure preexponential of Reaction 13 reduces the delay (faster combustion), whereas the high-pressure preexponential of Reaction 14 has the opposite effect.

(2) Based on the relative coefficient values of these reactions steps (Reactions 13 and 14), the $CH_3CH_2CH_2OO\cdot = CH_2\cdot CH_2CH_2OOH$ isomerization is critical at low temperature (second O_2 addition results in branching), whereas the HO_2 elimination is more important for the NTC.

(3) Analysis of the SRSM coefficients (Table 1) predicts that the expected variability, that is, impact, of high-pressure rate coefficients is most significant in the NTC regime, consistent with the sampling of the original model, which was used to develop Figure 8. The uncertainty propagation is less significant, but still large, in the low-temperature regime and its

Table 2. Linear SRSM Coefficients for the Propagation of Uncertainty from the Input Parameters of $C_3H_7 + O_2$ into the Ignition Delay of C_3H_8

No.	Description	Parameter	573 K	593 K	683 K
11	$n\text{-}C_3H_7\cdot + O_2 = C_3H_7OO\cdot$	A	−116.9	−204.2	31.2
12	$C_3H_7OO\cdot = CH_3CH\cdot CH_2OOH$	A	21.4	50.9	0.8
		E_a	−143.8	−292.4	−3.0
13	$C_3H_7OO\cdot = CH_2\cdot CH_2CH_2OOH$	A	**−376.0**	**−348.2**	**1.4**
		E_a	**1460.5**	**1250.5**	**5.7**
14	$C_3H_7OO\cdot = C_3H_6 + HO_2\cdot$	A	**2878.3**	**3864.0**	**52.2**
		E_a	**−2045.1**	**−8630.8**	**−110.1**
15	$C_3H_7OO\cdot = C_2H_5CHO + OH\cdot$	A	−0.1	1.3	0.2
		E_a	−1.9	−8.8	−0.1
16	$C_3H_7OO\cdot = C_3H_7O\cdot + O$	A	0.0	0.5	0.0
		E_a	−3.8	0.9	−0.6
17	$CH_3CH\cdot CH_2OOH = c\text{-}CH_3\ (C_2H_3O) + OH\cdot$	A	−17.6	−88.7	0.1
		E_a	38.1	184.6	2.9
18	$CH_3CH\cdot CH_2OOH = C_3H_6 + HO_2\cdot$	A	−11.3	−63.2	0.6
		E_a	23.0	128.5	1.7
19	$CH_2\cdot CH_2CH_2OOH = c\text{-}(C_3H_6O) + OH\cdot$	A	0.6	3.4	0.3
		E_a	−0.5	−5.2	0.0
20	$CH_2\cdot CH_2CH_2OOH = C_2H_4 + CH_2O + OH\cdot$	A	1.7	7.7	−0.6
		E_a	−2.3	−9.2	−3.4

significance decreases at the high-temperature regime. This is quantified by analyzing the expected standard deviation of the output. This can be either calculated from repeated simulations as in Figure 8 or estimated (Eq. 4).

(4) At high temperatures, most of the reactions of the peroxy radicals decrease in importance and their accuracy/variability has a diminished effect, as expected, in the macroscopic response of the system. Other reactions in the kinetic model, not included in the analysis, beyond those of the $n\text{-}C_3H_7 + O_2$ reaction, become dominant in the determination of the ignition delay (and are not included in Table 2). For example, the uncertainty in the initiation reaction $OH + C_3H_8 = n\text{-}C_3H_7 + H_2O$ has a greater impact on the uncertainty in the ignition delay at 683 K than any of the reactions listed in Table 2.

(5) Observations (1) and (2) are consistent with the current working hypothesis regarding the nature of NTC, according to which the HO_2 radicals are acting against chain branching because of their facile chain-terminating reactions

$$2HO_2 \rightarrow H_2O_2 + O_2$$

The results illustrate the need for accurate description of low-temperature kinetics because high-temperature phenomena can be described with very simplified chemical kinetics mechanisms and would completely miss the important pathways giving rise to low-temperature autoignition.

(6) The results of this analysis provide feedback and directions to improve the estimates of key parameters. For example, if one wanted to improve low-temperature ignition predictions, then the high-pressure estimates of Reactions 13 and 14 should be improved. Given that for Reactions 13 and 14 the SRSM coefficients are 10^2 to 10^4 larger than the corresponding coefficients of Reactions 12 and 15–20, one can assume that the other reactions are reasonably well characterized for this particular condition and macroscopic observable. If, on the other hand, one was interested in high-temperature oxidation, such as a flame, high-pressure parameters of Reactions 13 and 14 could be considered accurate, although quite possibly the high-pressure parameters of Reaction 16 could be uncertain, given that its rate coefficient increases with increasing temperature (and this reaction becomes the dominant pathway for this system at temperatures $\gtrsim$ 1200 K). This example illustrates the power of the method since we unraveled, in a systematic way, the highly nonlinear dependencies of the macroscopic observable to fundamental parameters such as high-pressure rate coefficients whose calculation depends on high-level theory ab initio calculations or any other estimation method.

Conclusions

We have developed and demonstrated a systematic methodology for quantifying the impact of uncertainty in the thermophysical parameters entering the complex calculation of fundamental kinetic parameters. This methodology allows identification of the expected ranges of variability of reaction rate coefficients when fundamental properties are known only approximately. The framework integrates uncertainty propagation models (SRSM), the chemical activation formalism, automated mechanism generation schemes, and reaction simulations and makes use of a reasonable number of model calculations for deriving approximate correlations between macroscopic observables, such as autoignition delay, and microscopic parameters, such as high-pressure rate coefficients.

Literature Cited

1. Miller JA, Klippenstein SJ. The reaction between ethyl and molecular oxygen. II: Further analysis. *Int J Chem Kinet.* 2001;33:654-668.
2. Barckholtz TA, Bozzelli JW, Chen C. Modeling the negative temperature coefficient in the low temperature oxidation of propane. Proceedings of the Third Joint Meeting of the U.S. Sections of the Combustion Institute, Chicago, IL, March 16–19; 2003.
3. Benson SW. *Thermochemical Kinetics.* New York, NY: Wiley; 1976.
4. Bozzelli JW, Dean AM. Chemical activation analysis of the reaction of C_2H_5 with O_2. *J Phys Chem.* 1990;94:3313-3317.
5. Ritter ER, Bozzelli JW. THERM: Thermodynamic property estimation for gas phase radicals and molecules. *Int J Chem Kinet.* 1991;23:767-778.
6. Westmoreland PR, Howard JB, Longwell JP, Dean AM. Prediction of rate coefficients for combustion and pyrolysis reactions by bimolecular QRRK. *AIChE J.* 1986;32:1971-1979.
7. Yamada T, Lay TH, Bozzelli JW. Ab-initio calculations and internal rotor contribution for thermodynamic properties $S_o(298)$ and $C_p(T)$: Group additivity for fluoroethanes. *J Phys Chem A.* 1998;102:7286-7293.
8. Sheng CY, Bozzelli JW, Dean AM, Chang AY. Detailed kinetics and thermochemistry of $C_2H_5 + O_2$: Reaction kinetics of the chemically activated and stabilized $CH_3CH_2OO^*$ adduct. *J Phys Chem A.* 2002; 106:7276-7293.
9. Kong SC, Reitz RD. Numerical study of premixed HCCI engine combustion and its sensitivity to computational mesh and model uncertainties. *Combust Theory Model.* 2003;7:417-433.
10. Chen CC, Bozzelli JW, Farrell JT. Thermochemical properties, pathways, and kinetic analysis on the reactions of benzene with OH: An elementary reaction mechanism. *J Phys Chem A.* 2004;108:4643-4652.
11. Rienstra-Kiracofe JC, Allen WD, Schaefer HF. The $C_2H_5 + O_2$ reaction mechanism: High-level ab initio characterization. *J Phys Chem.* 2000;104:9823-9840.
12. Dean AM. Development and application of detailed kinetic mechanisms for free radical systems. *AIChE Symp Ser.* 2001;97:84-95.
13. Green WH, Barton PI, Bhattacharjee B, Matheu DM, Schwer DA, Song BJ, Sumathi R, Castersen HH, Dean AM, Grenda JM. Computer construction of detailed chemical kinetic models for gas phase reactors. *Ind Eng Chem Res.* 2001;40:5362-5370.
14. Green WH, Wijaya CD, Yelvington PE, Sumathi R. Predicting chemical kinetics with computational chemistry: Is QOOH → HOQO important in fuel ignition? *Mol Phys.* 2004;102:371-380.
15. Grenda JM, Androulakis IP, Dean AM, Green WH. Application of computational kinetic mechanism generation to model the autocatalytic pyrolysis of methane. *Ind Eng Chem Res.* 2003;42:1000-1010.
16. Grenda JM, Dean AM, Peczak P, Green WH. Recent advances in the computational chemical kinetics mechanism generation techniques. Proceedings of the 27th International Symposium on Combustion, Boulder, CO, August 2–7; 1998.
17. Matheu DM, Dean AM, Grenda JM, Green WH. Mechanism generation with integrated pressure dependence: A new model for methane pyrolysis. *J Phys Chem A.* 2003;107:8552-8565.
18. Matheu DM, Green WH, Grenda JM. Capturing pressure-dependence in automated mechanism generation: Reactions through cycloalkyl intermediates. *Int J Chem Kinet.* 2003;35:95-119.
19. Matheu DM, Lada TA, Green WH, Dean AM, Grenda JM. Rate-based screening of pressure-dependent reaction networks. *Comput Phys Commun.* 2001;138:237-249.
20. Susnow RG, Dean AM, Green WH, Peczak P, Broadbelt LJ. Rate-based construction of kinetic models for complex systems. *J Phys Chem A.* 1997;101:3731-3740.
21. Holbrook KA, Pilling MJ, Robertson SH. *Unimolecular Reactions.* New York, NY: Wiley; 1996.
22. Carstensen HH, Naik CV, Dean AM. Detailed modeling of the reaction of $C_2H_5 + O_2$. *J Phys Chem A.* 2005;109:2264-2281.
23. Bozzelli JW, Chang AY, Dean AM. Molecular density of states from estimated vapor phase heat capacities. *Int J Chem Kinet.* 1997;29:161-170.
24. Chang AY, Bozzelli JW, Dean AM. Kinetic analysis of complex

chemical activated and unimolecular dissociation reactions with QRRK theory and the modified strong collision approximation. *Z Phys Chem.* 2000;214:1533-1568.
25. Dean AM. Predictions of pressure and temperature effects upon radical addition and recombination reactions. *J Phys Chem.* 1985;89:4600-4608.
26. Dean AM, Westmoreland PR. Bimolecular QRRK analysis of methyl radical reactions. *Int J Chem Kinet.* 1987;19:207-228.
27. Dean AM, Bozzelli JW. CHEMACT: A computer code to estimate rate coefficients for chemically activated reactions. *Combust Sci Technol.* 1991;80:63-85.
28. Gilbert RG, Luther K, Troe J. Theory of unimolecular reactions in the fall-off range. *Ber Bunsen-Ges Phys Chem.* 1983;87:169-177.
29. Venkatesh PK, Chang AY, Dean AM, Cohen MH, Carr RW. Parameterization of pressure- and temperature-dependent kinetics in multiple well reactions. *AIChE J.* 1997;43:1331-1340.
30. Androulakis IP, Grenda JM, Bozzelli JW. Time-integrated element flux and sensitivity pointers for the analysis and reduction of complex kinetic mechanisms. *AIChE J.* 2004:50;2965-2970.
31. Sebbar N, Bozzelli JW, Bockhorn H. Thermochemical properties, rotation barriers and group additivity for unsaturated hydrocarbons and radicals resulting from reaction of vinyl and phenyl radicals systems with O_2. *J Phys Chem A.* 2005;109:2233-2253.
32. Bozzelli JW, Dean AM. Hydrocarbon radical reactions with O_2: Comparison of allyl, formyl, and vinyl to ethyl. *J Phys Chem.* 1997;97:4427-4441.
33. Rabitz H, Kramer M, Dacol D. Sensitivity analysis in chemical kinetics. *Annu Rev Phys Chem.* 1983;34:419-461.
34. Scire JJ, Dryer FL, Yetter RA. Comparison of global and local sensitivity techniques for rate coefficients determined using complex reaction mechanisms. *Int J Chem Kinet.* 2001;33:784-802.
35. Turanyi T. Applications of sensitivity analysis to combustion chemistry. *Reliab Eng Syst Safety.* 1997;57:41-48.
36. Dunker AM. Efficient calculation of sensitivity coefficients for complex atmospheric models. *Atmos Environ.* 1981;15:1155-1161.
37. Saltelli A, Tarantola S, Campolongo F, Ratto M. *Sensitivity Analysis in Practice: A Guide to Assessing Scientific Models.* Hoboken, NJ: Wiley; 2004.
38. Fishman GS. *Monte Carlo: Concepts, Algorithms, and Applications.* New York, NY: Springer-Verlag; 1996.
39. Loh WI. On Latin hypercube sampling. *Ann Stat.* 1996;24:2058-2080.
40. McRae GJ, Tilden JW, Seinfeld JH. Global sensitivity analysis—A computational implementation of the Fourier Amplitude Sensitivity Test (FAST). *Comput Chem Eng.* 1979;6:15-25.
41. Tatang MA, Pan W, Prinn RG, McRae GJ. An efficient method for parametric uncertainty analysis of numerical geophysical models. *J Geophys Res.* 1997;102:925-932.
42. Isukapalli SS, Roy A, Georgopoulos PG. Efficient sensitivity/uncertainty analysis using the combined stochastic response surface method and automated differentiation: Application to environmental and biological systems. *Risk Anal.* 2000;20:591-602.
43. Isukapalli SS, Roy A, Georgopoulos PG. Stochastic response surface methods (SRSMs) for uncertainty propagation: Application to environmental and biological systems. *Risk Anal.* 1998;18:351-363.
44. Phenix BD, Dinard JI, Tatang MA, Tester JW, Howard JB, McRae GJ. Incorporation of parametric uncertainty into complex mechanism: Application to hydrogen oxidation in supercritical water. *Combust Flame.* 1998;112:132-146.
45. Tatang MA. *Direct Incorporation of Uncertainty in Chemical and Environmental Engineering Systems*. Cambridge, MA: MIT Press; 1995.
46. Ghanem R, Spanos P. *Stochastic Finite Elements: A Spectral Approach.* New York, NY: Springer-Verlag; 1991.
47. Frenklach M, Packard A, Seiler P. Prediction uncertainty from models and data. Proceedings of the American Control Conference, Anchorage, AK, May 8–10; 2002.
48. Balakrishnan S, Georgopoulos P, Banerjee I, Ierapetritou MG. Uncertainty consideration for describing complex reaction systems. *AIChE J.* 2002;48:2875-2889.
49. Pilling MJ, Hancock G. *Low Temperature Combustion and Autoignition.* New York, NY: Elsevier; 1997.
50. Reagan MT, Ajm HN, Ghanem RG, Knio OK. Uncertainty quantification in reacting-flow simulations through non-intrusive spectral projections. *Combust Flame.* 2003;132:545-555.
51. Koert DN, Miller DL, Cernansky NP. Experimental studies of propane oxidation through the negative temperature coefficient region at 10 and 15 atmospheres. *Combust Flame.* 1994;96:34-49.

Manuscript received Dec. 7, 2005, and revision received Apr. 29, 2006.